Sciencexpress Research Articles

Abrupt warming events drove Late Pleistocene Holarctic megafaunal turnover

Alan Cooper,[1]* Chris Turney,[2]* Konrad A. Hughen,[3] Barry W. Brook,[4,5] H. Gregory McDonald,[6] Corey J. A. Bradshaw[4]

[1]Australian Centre for Ancient DNA, School of Earth and Environmental Sciences, and Environment Institute, University of Adelaide, Adelaide, Australia. [2]Climate Change Research Centre and School of Biological, Earth, and Environmental Sciences, University of New South Wales, Sydney, Australia. [3]Woods Hole Oceanographic Institution, Woods Hole, MA 02543, USA. [4]Environment Institute and School of Biological Sciences, University of Adelaide, Adelaide, Australia. [5]School of Biological Sciences, University of Tasmania, Hobart, Australia. [6]Museum Management Program, National Parks Service, Fort Collins, CO 80525, USA.

*Corresponding author. E-mail: alan.cooper@adelaide.edu.au (A.C.); c.turney@unsw.edu.au (C.T.)

The mechanisms of Late Pleistocene megafauna extinctions remain fiercely contested, with human impact or climate change cited as principal drivers. Here, we compare ancient DNA and radiocarbon data from 31 detailed time series of regional megafaunal extinctions/replacements over the past 56,000 years with standard and new combined records of Northern Hemisphere climate in the Late Pleistocene. Unexpectedly, rapid climate changes associated with interstadial warming events are strongly associated with the regional replacement/extinction of major genetic clades or species of megafauna. The presence of many cryptic biotic transitions prior to the Pleistocene/Holocene boundary revealed by ancient DNA confirms the importance of climate change in megafaunal population extinctions and suggests that metapopulation structures necessary to survive such repeated and rapid climatic shifts were susceptible to human impacts.

The debate surrounding the causes of the extinctions of megafaunal species (terrestrial taxa with adults > 45 kg), which occurred during the last glacial period (ca. 110,000-11,650 calendar years ago; 110-11.65 kyr) in the Late Pleistocene, has continued for over two centuries since Cuvier first identified the mammoth and giant ground sloth (*1–5*). While human activity as a result of hunting ("overkill") and/or habitat modification and fragmentation are often cited as the principal driving force (*1*, *6–8*), the diversity of extinction patterns observed on different continents has led to increasing recognition of the potential synergistic role of climate change (*1–4*, *9*). A major confounding factor in the debate has been the coincident Late Pleistocene increase in human population size and migration into previously uninhabited areas, such as the New World, potentially exacerbating other ecological impacts.

Traditionally, a key argument against the potential role of climate-change impacts has been the paucity of identified extinction events during either previous glacial cycles or the many well-defined, climatic shifts recorded during the last glacial period (*3*, *4*), including the Last Glacial Maximum (LGM; ca. 23-19 kyr) (Fig. 1). However, the lack of suitably resolved records of climate change and radiocarbon calibration on a common timescale makes such interpretations particularly challenging. The debate has also been constrained by the heavy reliance on fossil morphological evidence, precluding the identification of major genetic transitions or population-level turnovers, Recent work using ancient DNA (aDNA) has shown that morphological analyses of the Pleistocene palaeontological record can have limited power to resolve species-level mammalian taxonomy issues or detect broad-scale genetic transitions at the population level, even when species suffer major genetic losses or almost go extinct (*10–15*). Indeed, aDNA and genomic studies have revealed a far more dynamic picture of megafaunal population ecology, including repeated localized extinctions, migrations and replacements (*10*, *12–15*).

The Late Pleistocene was characterized by a series of severe and rapid climate oscillations (regional temperature changes of up to 16°C) known as Dansgaard-Oeschger (D-O) events that have been identified in oceanic, ice and terrestrial records throughout the Northern Hemisphere (*16*) (Fig. 1 and fig. S3). The millennial-length D-O events can be bundled into semi-regular cooling cycles with an asymmetrical "saw-tooth" pattern (Bond Cycles) (*17*) that culminate in massive discharges of ice into the North Atlantic, known as Heinrich events. However, the precise timing, magnitude, and global extent of these events remain sufficiently uncertain to impair research into the effects of such rapid and extreme climate shifts on landscape and paleoecological change. In particular, there has been limited analysis of the potential relationship between rapid climate change and major genetic transitions in widespread populations, marked by local extirpations or global extinctions of species and genetic diversity.

Megafaunal data

To investigate this, we examined all available megafaunal species with comprehensive radiocarbon-dated series, and plotted 31 calibrated major megafaunal transition events (defined as geographically widespread or global extinctions, or invasions, of species or major clades) that have been de-

tected in either genetic (13 events) or palaeontological (18 events) studies against the Greenland ice core record (on the GICC05 timescale) (*18*–*20*) (Fig. 1).

The genetic and radiocarbon data reveal a temporally staggered, long-term dynamic record of major megafaunal transitions across species with diverse ecologies and life histories. The events were widely distributed geographically across both Eurasia and the New World and included periods prior to human invasion. Multiple events appear to involve the rapid replacement of one species or population by a conspecific or congeneric across a broad area, often making the events undetectable in the fossil record on the basis of morphology, and potentially even to low-resolution genetic reconstructions of population palaeodemography (*21*). These rapid replacements suggest that putative taphonomic biases (e.g., increased fossilization rates during either interstadials or stadials) are not responsible for the apparent sudden disappearance/appearance of genetic diversity. Furthermore, common megafaunal fossils such as mammoth appear throughout the time period examined (Fig. 1). The apparent absence of extinctions during the cold conditions of the LGM, when Northern Hemisphere ice sheets reached their maximum volume, or to a lesser extent during the Younger Dryas stadial (11.7-12.7 kyr) (table S3) at the very end of the Pleistocene, is surprising given these events are commonly postulated as potential causes of megafaunal extinctions (*3*, *22*). While palaeontological studies record range contractions into glacial refugia for many species during this period (*4*), it appears that in general, cold conditions were not an important driver for extinctions even in the presence of anatomically modern humans in Europe.

The megafaunal transitions appear to be centered around D-O warming (interstadial) events leading up to and then following the LGM, including a marked cluster of events around interstadials 5-7 in northern Europe (ca. 37-32 kyr) (Fig. 1). A further well-known cluster of extinction events occurs during the termination of the Pleistocene (ca. 14-11 kyr), which has often been linked to the initial entry of humans into the New World (ca. 15 kyr) (*6*–*8*). However, half of the 12 extinction events in this period occur in western Eurasia where modern humans arrived at least ca. 44 kyr. Indeed, several taxa (e.g., mammoth) go extinct on the mainland of Eurasia considerably later than that of the New World, despite a much longer exposure to human hunting (*3*, *4*) (Fig. 1).

Greenland-Cariaco climate timescale

A major challenge for testing whether the genetic transitions were synchronous with D-O events is the placement of megafaunal and climate records on a common timescale (*23*). While the Greenland ice cores (*18*, *19*) provide a detailed record of climate change for the North Atlantic, cumulative counting errors can exceed 2% [fig. S1 (*20*)], resulting in calendar timescale offsets of up to 1,000 years between Greenland D-O events and radiocarbon calibrated megafaunal transitions (*23*, *24*). To enable detailed comparisons, the climate and radiocarbon records should be on the same absolute timescale, which requires the merging of different high-resolution datasets. Importantly, this also provides a means to improve the accuracy and precision of the chronological framework and to assess the hemispheric nature of the climate shifts. One such approach is to use the abrupt shifts at the onset of D-O warming as tie points to correlate across multiple climate records (*25*), because these events caused widespread and rapid climate effects by decreasing the Northern Hemisphere temperature gradient (*26*), resulting in a poleward migration of the Intertropical Convergence Zone (ITCZ) and associated changes in tropical rainfall belts (*27*–*31*). In this regard, a key record is the Venezuelan Cariaco Basin marine sequence which captures a climate record via shifts in the trade winds associated with northward migration of the ITCZ in the tropical Atlantic (*20*, *28*), alongside a comprehensive suite of radiocarbon ages from planktonic foraminifera in the sediment core. The Cariaco sediments are annually laminated during the Late-glacial and Holocene, providing independent age control from 14.7 kyr (*32*) prior to which distinct millennial-scale variability in sedimentological and geochemical proxies has been robustly correlated with the uranium series-dated Hulu Cave $\delta^{18}O$ speleothem record (with age uncertainties < 1%) (*33*).

We therefore used a D-O event tie-point approach to combine the calendar-age estimates obtained from Cariaco Basin (*28*) with the same interstadial events recorded in Greenland to allow direct comparison between radiocarbon-dates and climate change, thereby allowing us to test the apparent association between megafaunal extinction/replacement with warming events (Fig. 1). We find the timing of onsets of interstadial warming events in the two records to be statistically identical (*20*) allowing us to use OxCal 4.1 (*34*) to combine the two chronologies, and merge the calendar-dated onset of each interstadial in Cariaco with the annual layer-counted interstadial onset and duration from Greenland to generate a new combined record of the timing and duration of abrupt and extreme swings of north Atlantic temperature during the past 56 kyr (Fig. 1) (*20*) (tables S3 and S4). Our new reconstruction shows that while all current estimates of the onset of interstadial events in the GICC05 $\delta^{18}O$ record are within the errors of our combined Cariaco-Greenland chronology, the uncertainty surrounding these transitions is greatly reduced (by 18-79%) (Fig. 1, table S3, and figs. S2 and S4).

Testing climate-extinction associations

We used statistical resampling to test the distribution of megafaunal transitions for randomness relative to extreme and abrupt climatic events (either stadials or interstadials), using both the existing GICC05 and our new Cariaco-Greenland chronology (Fig. 1 and table S4) (*20*). We calculated the probability that the observed overlap between cli-

mate events and extinction/invasion events might be non-random by repeatedly randomizing the temporal position (but not duration) of the former and for each iteration, counting the number of times overlap was observed with the latter. To do this we used the calibrated radiocarbon age of the terminal observation of a clade/taxon (youngest age for extinctions, oldest for invasions), but also inferred unobserved temporal (ghost) ranges using the Gaussian-resampled, inverse-weighted McInerney (GRIWM) method (*20*, *35*), which incorporates both sampling density and dating errors to estimate the most plausible temporal range of last/first occurrence. A clear non-random relationship was observed between interstadial events and megafaunal transitions for both the terminal observations and GRIWM-based estimates, with statistical power depending on the number of transitions tested, but importantly no such non-random overlap was detected for stadials (Fig. 2 and Table 1 (*20*). It is notable that a non-random association is observed despite the uncertainties in the taphonomic, sampling, and dating processes involved in the datasets, but it is apparent with both the standard published GICC05 record and the new combined Cariaco-Greenland chronology (Table 1). A correlation can be seen even when terminal Pleistocene events are discarded to avoid the potential confounding impacts of human colonization (Fig. 2 and Table 1). The Younger Dryas stadial has also often been suggested as a prime climatic driver of extinctions (*3*, *4*, *22*), but even for this event the observed extinction events are distributed much more toward the preceding interstadial warm period (Fig. 1 and fig. S7), despite the larger dating uncertainties caused by radiocarbon plateaux at this time (*36*).

Interstadial impacts

The onsets of interstadials represent the most rapid and extreme changes observed in the Late Pleistocene climate record (Fig. 1) (*20*), and these are likely to have caused abrupt shifts in temperature or precipitation (either wetter or drier depending on local environments) away from a previous relatively stable state. These factors would have promoted changes in species ranges and distributions, potentially resulting in regional turnover. The local or regional expression of global climate variation (such as D-O events) is highly variable (*37*), and this is consistent with the megafaunal transition events being distributed broadly in terms of geography, taxonomy and age. This diffuse pattern, along with methodological limitations used in simple genetic paleodemographic reconstructions (*21*), might explain why correlations with climate events may have been difficult to detect previously. The lack of extinctions during the LGM is consistent with the stability of the climate during this period, albeit cold, in contrast with the large millennial-scale variability before and after, both of which coincide with high rates of extinctions.

The megafaunal taxa analyzed cover a wide range of life histories and ecological roles, and include forest and steppe taxa. Many species have a broad niche (e.g., *Ursus arctos*, *Bison* spp., Neandertals), making it difficult to classify taxa into cold- or warm-adapted groups as has previously been advocated (*3*, *4*, *38*). Furthermore, the rapid and drastic climate changes associated with both the onset and end of interstadials, followed by new climate regimes, are potentially sufficient to disrupt populations of taxa across a wide range of niches. The effects of high-amplitude climate change, followed by either stadial or interstadial conditions, is potentially compatible with previous suggestions that the extirpation of cold or open-adapted taxa such as woolly rhino and mammoth occurred during interstadials, and warm-adapted taxa such as the giant deer during stadials like the Younger Dryas (*38*). However, the widely dispersed temporal record of the megafaunal transitions suggests a markedly individualistic species response (*39*), presumably exaggerated by the localized environmental responses to climatic shifts (*37*). Simulations of paleovegetation patterns in the late Pleistocene have emphasized the importance of the duration and nature of interstadial events, and their impact on the growth of factors such as forests (*40*). In contrast, however, we observe a more pronounced relationship between short interstadials (IS 3-7) and megafaunal events, rather than with the longer interstadials, such as 8 and 12, which might have been expected to allow larger-scale changes in the extent and nature of forest cover.

Our results lend strong empirical support to the hypothesis that environmental changes associated with rapid climatic shifts were important factors in the extinction of many megafaunal lineages. Indeed, the rapid replacement of local genetic populations by congeners or conspecifics (e.g., cave bears, bison, mammoth) revealed by ancient DNA suggests that broader-scale metapopulation structures or processes (e.g., long-distance dispersal, refugia and rescue effects across spatially distributed subpopulations) were involved in maintaining ecosystem stability during the repeated phases of sudden climate change in the Pleistocene Holarctic. If so, human presence could have had a major and negative impact on megafaunal metapopulations by interrupting subpopulation connectivity, especially by concentrating on regular pathways between resource-rich zones (*1*), potentially leaving minimal signs of direct hunting. By interrupting metapopulation processes (e.g., dispersal, recolonization), humans could have both exacerbated regional extinctions brought on by climate changes and allowed them to coalesce, potentially leading to the eventual regime shifts and collapses observed in megafaunal ecosystems. The lack of evidence for larger-scale ecological regime shifts during earlier periods of the Glacial (i.e., >45 kyr) when interstadial events were common, but humans were not, supports a synergistic role for humans in exacerbating the impacts of climate change and extinction in the terminal events.

REFERENCES AND NOTES

1. G. Haynes, Extinctions in North America's Late Glacial landscapes. *Quat. Int.* **285**, 89–98 (2013). doi:10.1016/j.quaint.2010.07.026
2. R. D. Guthrie, New carbon dates link climatic change with human colonization and Pleistocene extinctions. *Nature* **441**, 207–209 (2006). Medline doi:10.1038/nature04604
3. P. L. Koch, A. D. Barnosky, Late Quaternary extinctions: State of the debate. *Annu. Rev. Ecol. Evol. Syst.* **37**, 215–250 (2006). doi:10.1146/annurev.ecolsys.34.011802.132415
4. A. J. Stuart, A. M. Lister, Extinction chronology of the woolly rhinoceros *Coelodonta antiquitatis* in the context of late Quaternary megafaunal extinctions in northern Eurasia. *Quat. Sci. Rev.* **51**, 1–17 (2012). doi:10.1016/j.quascirev.2012.06.007
5. G. Cuvier, Notice sur le squellette d'une très grande espèce de quadrupède inconnue jusqu'à présent, trouvé au Paraquay, et déposé au cabinet d'histoire naturelle de Madrid. *Magasin* encyclopédique, ou *Journal des Sciences, des Lettres et des Arts*, vol. 1, pp. 303–310 and vol. 2, pp. 227–228 (1796).
6. P. S. Martin, "Prehistoric overkill: The global model," in *Quaternary Extinctions: A Prehistoric Revolution*, P. S. Martin, R. D. Klein, Eds. (Univ. Arizona Press, Tucson, AZ, 1984).
7. J. Diamond, Quaternary megafaunal extinctions: Variations on a theme by Paganini. *J. Archaeol. Sci.* **16**, 167–175 (1989). doi:10.1016/0305-4403(89)90064-2
8. J. Alroy, A multispecies overkill simulation of the end-Pleistocene megafaunal mass extinction. *Science* **292**, 1893–1896 (2001). Medline doi:10.1126/science.1059342
9. E. D. Lorenzen, D. Nogués-Bravo, L. Orlando, J. Weinstock, J. Binladen, K. A. Marske, A. Ugan, M. K. Borregaard, M. T. Gilbert, R. Nielsen, S. Y. Ho, T. Goebel, K. E. Graf, D. Byers, J. T. Stenderup, M. Rasmussen, P. F. Campos, J. A. Leonard, K. P. Koepfli, D. Froese, G. Zazula, T. W. Stafford Jr., K. Aaris-Sørensen, P. Batra, A. M. Haywood, J. S. Singarayer, P. J. Valdes, G. Boeskorov, J. A. Burns, S. P. Davydov, J. Haile, D. L. Jenkins, P. Kosintsev, T. Kuznetsova, X. Lai, L. D. Martin, H. G. McDonald, D. Mol, M. Meldgaard, K. Munch, E. Stephan, M. Sablin, R. S. Sommer, T. Sipko, E. Scott, M. A. Suchard, A. Tikhonov, R. Willerslev, R. K. Wayne, A. Cooper, M. Hofreiter, A. Sher, B. Shapiro, C. Rahbek, E. Willerslev, Species-specific responses of Late Quaternary megafauna to climate and humans. *Nature* **479**, 359–364 (2011). Medline doi:10.1038/nature10574
10. I. Barnes, P. Matheus, B. Shapiro, D. Jensen, A. Cooper, Dynamics of Pleistocene population extinctions in Beringian brown bears. *Science* **295**, 2267–2270 (2002). Medline doi:10.1126/science.1067814
11. M. Bunce, T. H. Worthy, T. Ford, W. Hoppitt, E. Willerslev, A. Drummond, A. Cooper, Extreme reversed sexual size dimorphism in the extinct New Zealand moa *Dinornis*. *Nature* **425**, 172–175 (2003). Medline doi:10.1038/nature01871
12. B. Shapiro, A. J. Drummond, A. Rambaut, M. C. Wilson, P. E. Matheus, A. V. Sher, O. G. Pybus, M. T. Gilbert, I. Barnes, J. Binladen, E. Willerslev, A. J. Hansen, G. F. Baryshnikov, J. A. Burns, S. Davydov, J. C. Driver, D. G. Froese, C. R. Harington, G. Keddie, P. Kosintsev, M. L. Kunz, L. D. Martin, R. O. Stephenson, J. Storer, R. Tedford, S. Zimov, A. Cooper, Rise and fall of the Beringian steppe bison. *Science* **306**, 1561–1565 (2004). Medline doi:10.1126/science.1101074
13. M. Hofreiter, J. Stewart, Ecological change, range fluctuations and population dynamics during the Pleistocene. *Curr. Biol.* **19**, R584–R594 (2009). Medline doi:10.1016/j.cub.2009.06.030
14. W. Miller, S. C. Schuster, A. J. Welch, A. Ratan, O. C. Bedoya-Reina, F. Zhao, H. L. Kim, R. C. Burhans, D. I. Drautz, N. E. Wittekindt, L. P. Tomsho, E. Ibarra-Laclette, L. Herrera-Estrella, E. Peacock, S. Farley, G. K. Sage, K. Rode, M. Obbard, R. Montiel, L. Bachmann, O. Ingólfsson, J. Aars, T. Mailund, O. Wiig, S. L. Talbot, C. Lindqvist, Polar and brown bear genomes reveal ancient admixture and demographic footprints of past climate change. *Proc. Natl. Acad. Sci. U.S.A.* **109**, E2382–E2390 (2012). Medline doi:10.1073/pnas.1210506109
15. S. Brace, E. Palkopoulou, L. Dalén, A. M. Lister, R. Miller, M. Otte, M. Germonpré, S. P. Blockley, J. R. Stewart, I. Barnes, Serial population extinctions in a small mammal indicate Late Pleistocene ecosystem instability. *Proc. Natl. Acad. Sci. U.S.A.* **109**, 20532–20536 (2012). Medline doi:10.1073/pnas.1213322109
16. E. W. Wolff, J. Chappellaz, T. Blunier, S. O. Rasmussen, A. Svensson, Millennial-scale variability during the last glacial: The ice core record. *Quat. Sci. Rev.* **29**, 2828–2838 (2010). doi:10.1016/j.quascirev.2009.10.013
17. G. Bond, W. Broecker, S. Johnsen, J. McManus, L. Labeyrie, J. Jouzel, G. Bonani, Correlations between climate records from North Atlantic sediments and Greenland ice. *Nature* **365**, 143–147 (1993). doi:10.1038/365143a0
18. S. O. Rasmussen, K. K. Andersen, A. M. Svensson, J. P. Steffensen, B. M. Vinther, H. B. Clausen, M.-L. Siggaard-Andersen, S. J. Johnsen, L. B. Larsen, D. Dahl-Jensen, M. Bigler, R. Röthlisberger, H. Fischer, K. Goto-Azuma, M. E. Hansson, U. Ruth, A new Greenland ice core chronology for the last glacial termination. *J. Geophys. Res.* **111**, D06102 (2006). doi:10.1029/2005JD006079
19. A. Svensson, K. K. Andersen, M. Bigler, H. B. Clausen, D. Dahl-Jensen, S. M. Davies, S. J. Johnsen, R. Muscheler, F. Parrenin, S. O. Rasmussen, R. Röthlisberger, I. Seierstad, J. P. Steffensen, B. M. Vinther, Greenland stratigraphic ice core chronology. *Climate of the Past* **4**, 47–57 (2008). doi:10.5194/cp-4-47-2008
20. See the supplementary materials available on *Science* Online.
21. T. Mourier, S. Y. Ho, M. T. Gilbert, E. Willerslev, L. Orlando, Statistical guidelines for detecting past population shifts using ancient DNA. *Mol. Biol. Evol.* **29**, 2241–2251 (2012). Medline doi:10.1093/molbev/mss094
22. G. M. MacDonald, D. W. Beilman, Y. V. Kuzmin, L. A. Orlova, K. V. Kremenetski, B. Shapiro, R. K. Wayne, B. Van Valkenburgh, Pattern of extinction of the woolly mammoth in Beringia. *Nat. Commun.* **3**, 893 (2012). Medline doi:10.1038/ncomms1881
23. R. Muscheler, F. Adolphi, A. Svensson, Challenges in ^{14}C dating towards the limit of the method inferred from anchoring a floating tree ring radiocarbon chronology to ice core records around the Laschamp geomagnetic field minimum. *Earth Planet. Sci. Lett.* **394**, 209–215 (2014). doi:10.1016/j.epsl.2014.03.024
24. C. Buizert, K. M. Cuffey, J. P. Severinghaus, D. Baggenstos, T. J. Fudge, E. J. Steig, B. R. Markle, M. Winstrup, R. H. Rhodes, E. J. Brook, T. A. Sowers, G. D. Clow, H. Cheng, R. L. Edwards, M. Sigl, J. R. McConnell, K. C. Taylor, The WAIS Divide deep ice core WD2014 chronology; Part 1: Methane synchronization (68–31 ka BP) and the gas age–ice age difference. *Climate of the Past* **11**, 153–173 (2015). doi:10.5194/cp-11-153-2015
25. N. J. Shackleton, R. G. Fairbanks, T. C. Chiu, F. Parrenin, Absolute calibration of the Greenland time scale: Implications for Antarctic time scales and for Delta C-14. *Quat. Sci. Rev.* **23**, 1513–1522 (2004). 10.1016/j.quascirev.2004.03.006 doi:10.1016/j.quascirev.2004.03.006
26. J. T. Overpeck, L. C. Peterson, N. Kipp, J. Imbrie, D. Rind, Climate change in the circum-North Atlantic region during the last deglaciation. *Nature* **338**, 553–557 (1989). doi:10.1038/338553a0
27. K. A. Hughen, J. T. Overpeck, L. C. Peterson, S. Trumbore, Rapid climate changes in the tropical Atlantic region during the last deglaciation. *Nature* **380**, 51–54 (1996). doi:10.1038/380051a0
28. K. Hughen, J. Southon, S. Lehman, C. Bertrand, J. Turnbull, Marine-derived ^{14}C calibration and activity record for the past 50,000 years updated from the Cariaco Basin. *Quat. Sci. Rev.* **25**, 3216–3227 (2006). doi:10.1016/j.quascirev.2006.03.014
29. L. C. Peterson, G. H. Haug, K. A. Hughen, U. Röhl, Rapid changes in the hydrologic cycle of the tropical Atlantic during the last glacial. *Science* **290**, 1947–1951 (2000). Medline doi:10.1126/science.290.5498.1947
30. S. C. Porter, A. Zhisheng, Correlation between climate events in the North Atlantic and China during the last glaciation. *Nature* **375**, 305–308 (1995). doi:10.1038/375305a0
31. Y. Wang, H. Cheng, R. L. Edwards, X. Kong, X. Shao, S. Chen, J. Wu, X. Jiang, X. Wang, Z. An, Millennial- and orbital-scale changes in the East Asian monsoon over the past 224,000 years. *Nature* **451**, 1090–1093 (2008). Medline doi:10.1038/nature06692
32. K. A. Hughen, J. R. Southon, C. J. H. Bertrand, B. Frantz, P. Zermeño, Cariaco Basin calibration update: Revisions to calendar and 14C chronologies for core PL07-58PC. *Radiocarbon* **46**, 1161–1187 (2004). https://journals.uair.arizona.edu/index.php/radiocarbon/article/view/4175
33. T. J. Heaton, E. Bard, K. Hughen, Elastic tie-pointing—transferring chronologies between records via a Gaussian process. *Radiocarbon* **55**, 1975–1997 (2013). doi:10.2458/azu_js_rc.55.17777
34. C. B. Ramsey, Bayesian analysis of radiocarbon dates. *Radiocarbon* **51**, 337–360 (2009).
35. C. J. A. Bradshaw, A. Cooper, C. S. M. Turney, B. W. Brook, Robust estimates of extinction time in the geological record. *Quat. Sci. Rev.* **33**, 14–19 (2012). doi:10.1016/j.quascirev.2011.11.021
36. P. J. Reimer, E. Bard, A. Bayliss, J. W. Beck, P. G. Blackwell, C. Bronk Ramsey, C. E. Buck, H. Cheng, R. L. Edwards, M. Friedrich, P. M. Grootes, T. P. Guilderson, H.

Haflidason, I. Hajdas, C. Hatté, T. J. Heaton, D. L. Hoffmann, A. G. Hogg, K. A. Hughen, K. F. Kaiser, B. Kromer, S. W. Manning, M. Niu, R. W. Reimer, D. A. Richards, E. M. Scott, J. R. Southon, R. A. Staff, C. S. M. Turney, J. van der Plicht, IntCal13 and Marine13 radiocarbon age calibration curves 0–50,000 years cal BP. *Radiocarbon* **55**, 1869–1887 (2013). doi:10.2458/azu_js_rc.55.16947
37. X. A. S. Wang, A. S. Auler, R. L. Edwards, H. Cheng, E. Ito, Y. Wang, X. Kong, M. Solheid, Millennial-scale precipitation changes in southern Brazil over the past 90,000 years. *Geophys. Res. Lett.* **34**, L23701 (2007). doi:10.1029/2007GL031149
38. A. J. Stuart, P. A. Kosintsev, T. F. G. Higham, A. M. Lister, Pleistocene to Holocene extinction dynamics in giant deer and woolly mammoth. *Nature* **431**, 684–689 (2004). Medline doi:10.1038/nature02890
39. J. R. Stewart, The evolutionary consequence of the individualistic response to climate change. *J. Evol. Biol.* **22**, 2363–2375 (2009). Medline doi:10.1111/j.1420-9101.2009.01859.x
40. B. Huntley, J. R. Allen, Y. C. Collingham, T. Hickler, A. M. Lister, J. Singarayer, A. J. Stuart, M. T. Sykes, P. J. Valdes, Millennial climatic fluctuations are key to the structure of last glacial ecosystems. *PLOS ONE* **8**, e61963 (2013). Medline doi:10.1371/journal.pone.0061963
41. P. C. Tzedakis, K. A. Hughen, I. Cacho, K. Harvati, Placing late Neanderthals in a climatic context. *Nature* **449**, 206–208 (2007). Medline doi:10.1038/nature06117
42. W. E. N. Austin, F. D. Hibbert, S. O. Rasmussen, C. Peters, P. M. Abbott, C. L. Bryant, The synchronization of palaeoclimatic events in the North Atlantic region during Greenland Stadial 3 (ca 27.5 to 23.3 kyr b2k). *Quat. Sci. Rev.* **36**, 154–163 (2012). doi:10.1016/j.quascirev.2010.12.014
43. F. Saltré, B. W. Brook, M. Rodríguez-Rey, A. Cooper, C. N. Johnson, C. S. M. Turney, C. J. A. Bradshaw, Uncertainties in dating constrain model choice for inferring extinction time from fossil records. *Quat. Sci. Rev.* **112**, 128–137 (2015). doi:10.1016/j.quascirev.2015.01.022
44. J. Southon, A. L. Noronha, H. Cheng, R. L. Edwards, Y. Wang, A high-resolution record of atmospheric ^{14}C based on Hulu Cave speleothem H82. *Quat. Sci. Rev.* **33**, 32–41 (2012). doi:10.1016/j.quascirev.2011.11.022
45. C. B. Ramsey, Deposition models for chronological records. *Quat. Sci. Rev.* **27**, 42–60 (2008). doi:10.1016/j.quascirev.2007.01.019
46. T. Higham, K. Douka, R. Wood, C. B. Ramsey, F. Brock, L. Basell, M. Camps, A. Arrizabalaga, J. Baena, C. Barroso-Ruíz, C. Bergman, C. Boitard, P. Boscato, M. Caparrós, N. J. Conard, C. Draily, A. Froment, B. Galván, P. Gambassini, A. Garcia-Moreno, S. Grimaldi, P. Haesaerts, B. Holt, M. J. Iriarte-Chiapusso, A. Jelinek, J. F. Jordá Pardo, J. M. Maíllo-Fernández, A. Marom, J. Maroto, M. Menéndez, L. Metz, E. Morin, A. Moroni, F. Negrino, E. Panagopoulou, M. Peresani, S. Pirson, M. de la Rasilla, J. Riel-Salvatore, A. Ronchitelli, D. Santamaria, P. Semal, L. Slimak, J. Soler, N. Soler, A. Villaluenga, R. Pinhasi, R. Jacobi, The timing and spatiotemporal patterning of Neanderthal disappearance. *Nature* **512**, 306–309 (2014). Medline doi:10.1038/nature13621
47. C. B. Ramsey, T. Higham, P. Leach, Towards high-precision AMS; progress and limitations. *Radiocarbon* **46**, 17–24 (2007).
48. C. S. M. Turney, R. G. Roberts, Z. Jacobs, Archaeology: Progress and pitfalls in radiocarbon dating. *Nature* **443**, E3, discussion E4 (2006). Medline doi:10.1038/nature05214
49. R. D. Guthrie, Rapid body size decline in Alaskan Pleistocene horses before extinction. *Nature* **426**, 169–171 (2003). Medline doi:10.1038/nature02098
50. A. Ugan, D. Byers, Geographic and temporal trends in proboscidean and human radiocarbon histories during the late Pleistocene. *Quat. Sci. Rev.* **26**, 3058–3080 (2007). doi:10.1016/j.quascirev.2007.06.024
51. G. K. Ward, S. R. Wilson, Wilson SR (1978) Procedures for comparing and combining radiocarbon age determinations: A critique. *Archaeometry* **20**, 19–31 (1978). doi:10.1111/j.1475-4754.1978.tb00208.x
52. D. Rind, Relating paleoclimate data and past temperature gradients: Some suggestive rules. *Quat. Sci. Rev.* **19**, 381–390 (2000). doi:10.1016/S0277-3791(99)00070-0
53. D. Paillard, L. Labeyrie, P. Yiou, A Macintosh program that performs time-series analysis. *Eos Trans. AGU* **77**, 379 (1996). doi:10.1029/96EO00259
54. R. B. Firestone, A. West, J. P. Kennett, L. Becker, T. E. Bunch, Z. S. Revay, P. H. Schultz, T. Belgya, D. J. Kennett, J. M. Erlandson, O. J. Dickenson, A. C. Goodyear, R. S. Harris, G. A. Howard, J. B. Kloosterman, P. Lechler, P. A. Mayewski, J. Montgomery, R. Poreda, T. Darrah, S. S. Hee, A. R. Smith, A. Stich, W. Topping, J. H. Wittke, W. S. Wolbach, Evidence for an extraterrestrial impact 12,900 years ago that contributed to the megafaunal extinctions and the Younger Dryas cooling. *Proc. Natl. Acad. Sci. U.S.A.* **104**, 16016–16021 (2007). Medline doi:10.1073/pnas.0706977104

ACKNOWLEDGMENTS

We thank the following museums and curators for assistance with samples, advice, and encouragement: Canadian Museum of Nature (D. Harington), American Museum of Natural History (R. Tedford), Natural History Museum London (A. Currant), Yukon Heritage Centre (J. Storer, G. Zazula), University of Alaska, Fairbanks (D. Guthrie), Institute of Plant and Animal Ecology, RAS Yekaterinburg (P. Kosintsev and A. Vorobiev), Laboratory of Prehistory, St Petersburg (V. Doronichev and L. Golovanova); D. Froese, P. Matheus, T. Higham, A. Sher, J. Glimmerveen, B. Shapiro, T. Gilbert, E. Willerslev, R. Barnett, Yukon miners (B. Johnson, Ron Johnson, The Christie family, K. Tatlow, S. Schmidt), and L. Dalen and J. Soubrier for data and assistance. This work was supported by NSF NESCENT workshop "Integrating datasets to investigate megafaunal extinction in the late Quaternary." A.C., C.T., B.W.B., and C.J.A.B. were supported by Australian Research Council Federation, Laureate and Future Fellowships. The new GICCO5-Cariaco Basin $\delta^{18}O$ record is provided in the supplementary materials (*20*) and also lodged on the Paleoclimatology Database (NOAA). The previously published radiocarbon data, with original references, is presented in the supplementary materials (*20*). A.C. and C.T. conceived and performed research; A.C., C.J.A.B., C.T., and B.W.B. designed methods and performed analysis; A.C. and C.T. wrote the paper with input from all authors.

SUPPLEMENTARY MATERIALS

www.sciencemag.org/cgi/content/full/science.aac4315/DC1
Materials and Methods
Supplementary Text
Figs. S1 to S8
Tables S1 to S4
References (*43*–*54*)

27 April 2015; accepted 3 July 2015
Published online 23 July 2015
10.1126/science.aac4315

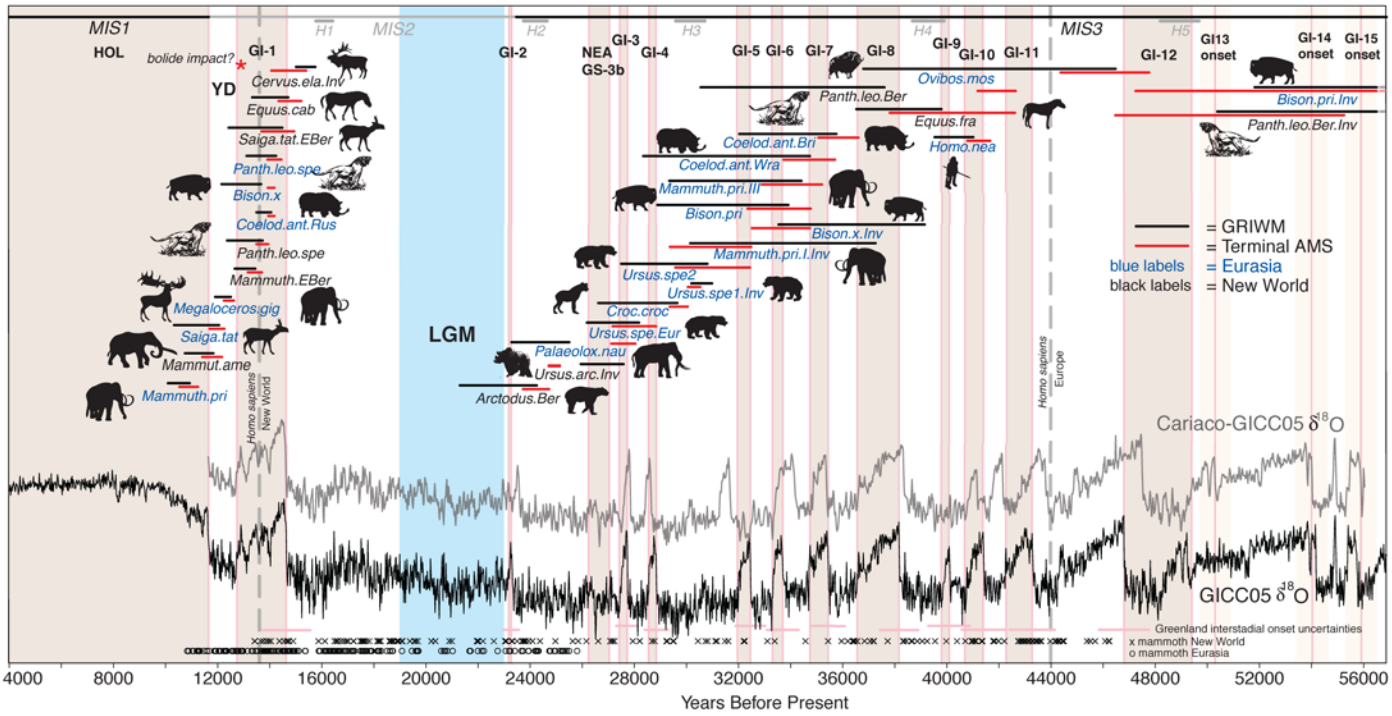

Fig. 1. Megafaunal transition events and Late Pleistocene climate records. Major megafaunal transition events (region-wide extirpations or global extinctions, or invasions, of species or major clades) identified in Late Pleistocene Holarctic megafaunal datasets through ancient DNA or paleontological studies, plotted on a reconstruction of Northern Hemisphere climate from the Greenland ice core (GICC05) $\delta^{18}O$ record (black wiggle curve). GICC05 interstadial (IS) warming events are shown with light grey boxes. There is an apparent absence of megafaunal events during the Last Glacial Maximum (LGM; blue) and to a lesser extent, the cold Younger Dryas stadial (YD), and a marked association with interstadials. AMS radiocarbon dates (red bar ± 2 sd, using *Phase* calibration in OxCal 4.1) calibrated using the dendro-dated IntCal <12.5ky dataset (*36*), and Cariaco Basin (Hulu Cave) dataset for older ages (*28*, *33*), or GRIWM-based estimates of ghost ranges (black bar, 95% confidence interval) are given for each event (*20*). Eurasian taxa are shown in blue and New World in black, with animals facing right representing extinctions and those facing left representing invasions (.Inv). The chronologically revised Greenland record, developed by combining the Cariaco Basin and Greenland ice core records, is also shown (dark grey wiggle curve) for the period >11.5ky (as it is identical with GICC05 until this point) (*20*). Light pink bars (below) represent the error margins (1 sd) for the estimated onset of GI events in the published GICC05 chronology (*19*, *20*). Heinrich events (H*x*) are shown with marine isotope stages (MIS*x*) in light grey at top (*41*). NEA-GS-3b was identified via Atlantic marine sediment cores and radiocarbon dating (*42*). Calibrated radiocarbon ages (midpoints without laboratory dating errors) from mammoth remains in Eurasia (black circles) and New World (crosses) are plotted across the bottom of the figure to demonstrate the lack of obvious taphonomic hiatus during the time period analyzed (*20*). The approximate timing of the first presence of modern humans in North America (New World) and Europe are shown as vertical grey dashed lines. Abbreviated taxonomic names, with geographic area appended where necessary, are given: *Arctodus.Ber* (*Arctodus simus* East Beringia); *Bison.pri* (*Bison priscus* Europe); *Bison.x* (*Bison* n. sp. Europe); *Cervus.ela* (*Cervus elephas* New World); *Coelod.ant.Bri* (*Coelodonta antiquitatis* Britain); *Coelod.ant.Rus* (*Coelodonta antiquitatis* Russia); *Coelodonta.ant.Wra* (*Coelodonta antiquitatis* Wrangel Island); *Croc.croc* (*Crocuta crocuta spelaea* Europe); *Equus.cab* (*Equus caballus* East Beringia); *Equus.fra* (*Equus francisci* East Beringia); *Homo.nea* (*Homo neanderthalensis* Europe); *Mammuth.pri* (*Mammuthus primigenius*); *Mammut.ame* (*Mammut americanum*); *Megaloceros.gig* (*Megaloceros giganteus* Western Europe); *Ovibos.mos* (*Ovibos moschatus* Beringia); *Palaeolox.nau* (*Palaeoloxodon naumanni* Japan); *Panth.leo.Ber* (*Panthera leo spelaea* Beringia); *Panth.leo.spe* (*Panthera leo spelaea* Eurasia); *Saiga.tat* (Saiga tatarica Eurasia); *Ursus.arc* (*Ursus arctos* East Beringia); *Ursus.spe1 and 2* (*Ursus spelaea* Germany); *Ursus.spe.Eur* (*Ursus spelaea* Europe). Further details of the geographic region and nature of each megafaunal event are presented in tables S1 and S2.

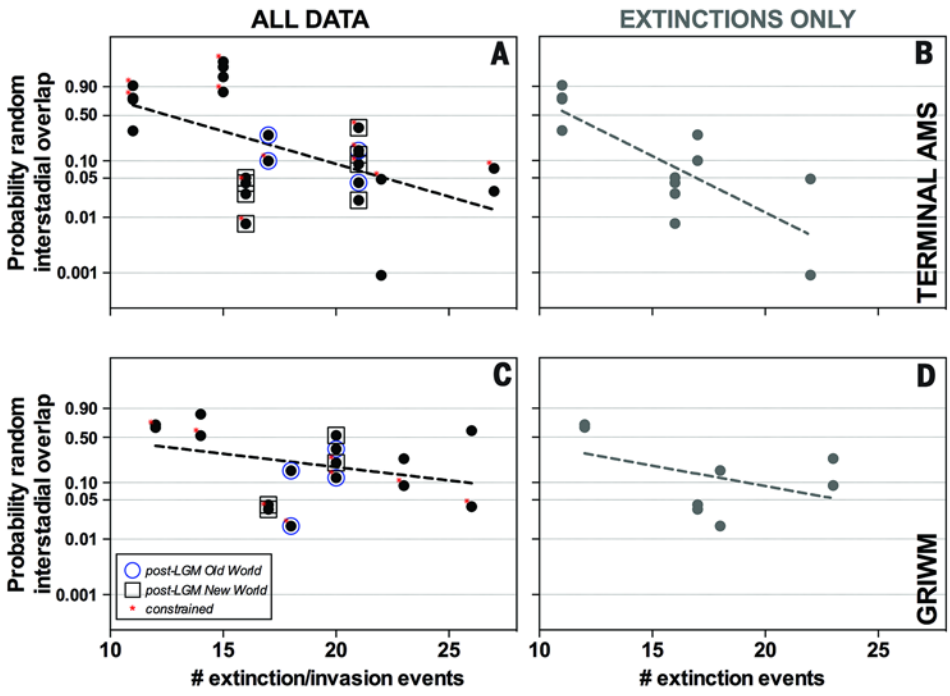

Fig. 2. Randomization tests of the timing of megafaunal transitions with interstadial events. Graphical representation of the simulation results presented in Table 1. The trend lines (dashed lines) show that the probability of generating the observed overlaps of megafaunal transition events with interstadials randomly (*P*) is inversely related to the number of events examined, while in contrast the probabilities for stadials were all > 0.60 (Table 1) (*20*). A strong correlation (steep gradient) was observed between megafaunal transitions (extinctions/invasion events) and interstadials using both: (top row; panels **A** and **B**) terminal AMS ^{14}C dates and (bottom row; panels **C** and **D**) GRIWM estimates (which use a statistical model of extinction times, based on a time series of records). The correlation was observed using either the GICC05 (shown), or new combined Cariaco-Greenland (Table 1 and fig. S6), chronologies. The plotted data are from simulations excluding events with wide confidence intervals, as inclusion nearly always resulted in a greater chance of overlap being random (i.e., higher *P* values, see *20*). To explore the effect of different combinations of megafaunal-transition events, certain subsets were removed and the simulations repeated: (i) excluding invasion events (right-hand panels B, D)—resulting in lower *P* of randomness; (ii) with a constrained-range overlap (red *) applied to reduce error margins around an event where a rapid replacement by a congener or conspecific was observed (*20*)—producing little difference in the results; and (iii) with post-LGM events from either the New World (○) or Eurasia (□) only (to remove the potential effects of terminal Pleistocene human-associated impacts)—where low *P* were observed, but sample-size constraints limited the number of simulations able to detect non-random interstadial overlap (*20*). The results of these additional simulations are distributed along most of the power relationship, suggesting the correlations are not driven by any particular grouped subset of the data.

Table 1. **Randomization tests of the timing of megafaunal transitions with major climate events.** Randomization tests of the timing of major megafaunal transitions with either interstadial or stadial events on the existing GICC05 and new combined Cariaco-Greenland timescales (*20*). The probabilities of generating the observed overlaps of extinction/invasion events at random with interstadials (P(rand) interstadials), and stadials (P(rand) stadials), are shown for both GRIWM and the Phase-calibrated terminal AMS dates, along with probabilities expressed on the complementary log-log scale. The correlation tests revealed non-random overlap relationships between the number of events *n* and interstadials for both the GICC05 and Cariaco-Greenland timescales. In contrast, probabilities for overlaps at random with stadial events were > 0.6 for both GRIWM and terminal AMS dates. Simulations producing low probabilities of generating the pattern of overlaps at random are cumulatively highlighted with asterisks ($P < 0.1$), in bold ($P < 0.05$), and in italics ($P < 0.01$). The power relationships for correlations with the GICC05 timescale are shown in Fig. 2. Simulations including terminal Pleistocene events from only the New World (NW) or Eurasia (Eur.) or neither (Pre-LGM) were used to explore the potentially confounding influences of human impact. Simulations using extinctions only (Extns) are indicated. The GICC05 timescale did not include interstadial NEA-GS-3b (table S3) as it is not detected in ice core records (*42*).

Events (Eurasia, New World)	Extinctions / Invasions	Muskox	Wide-CI species	Constrained range overlaps	Number of events (*n*) GRIWM	Number of events (*n*) Terminal AMS	Interstad P(random) GRIWM	Interstad P(random) Terminal AMS	Stadial P(random) GRIWM	Stadial P(random) Terminal AMS	Interstad P(random) GRIWM	Interstad P(random) Terminal AMS	Stadial P(random) GRIWM	Stadial P(random) Terminal AMS
							GICC05 chronology (19, 20)				*Cariaco-Greenland chronology*			
All	All	✓	✓	✓	28	29	**0.031**	0.228	0.801	0.999	0.126	0.220	0.998	0.998
All	All	✓	✓	✗	28	29	0.109	0.009*	0.995	0.999	0.470	0.082*	0.989	0.999
All	All	✗	✓	✓	27	28	**0.024**	**0.020**	0.974	0.997	0.066*	0.091*	0.983	0.996
All	All	✗	✗	✓	21	27	**0.038**	0.075*	0.994	0.975	0.252	0.117	0.998	0.995
All	All	✗	✗	✗	21	27	0.600	**0.030**	0.992	0.999	0.487	**0.037**	0.988	0.999
All	Extns	✓	✓	✗	24	23	0.296	***0.005***	0.999	0.992	0.396	**0.023**	0.999	0.999
All	Extns	✗	✓	✗	22	22	0.097*	0.026	0.994	0.974	0.302	**0.031**	0.999	0.999
All	Extns	✗	✓	✓	22	22	0.107	***0.001***	0.965	0.999	0.023	0.069*	0.999	0.997
All	Extns	✗	✗	✓	18	21	0.089*	**0.048**	0.999	0.999	0.131	0.087*	0.994	0.999
All	Extns	✗	✗	✗	18	21	0.249	***0.001***	0.999	0.999	0.287	***0.007***	0.999	0.999
Eur.	All	✓	✓	✓	22	24	**0.018**	0.230	0.985	0.897	0.414	0.529	0.998	0.914
Eur.	All	✓	✓	✗	23	24	0.453	**0.046**	0.977	0.999	0.425	0.161	0.996	0.950
Eur.	All	✗	✓	✗	22	23	0.227	0.088*	0.962	0.822	0.250	0.164	0.994	0.980
Eur.	All	✗	✓	✓	22	23	**0.040**	0.105	0.958	0.864	**0.019**	0.245	0.982	0.958
Eur.	All	✗	✗	✓	16	22	0.122	0.150	0.997	0.855	0.125	0.324	0.981	0.971
Eur.	All	✗	✗	✗	16	22	0.347	**0.042**	0.996	0.958	0.137	**0.022**	0.986	0.987
Eur.	Extns	✗	✓	✓	17	17	0.283	0.160	0.999	0.964	0.252	0.116	0.998	0.977
Eur.	Extns	✗	✗	✓	13	16	**0.017**	0.100*	0.985	0.991	0.073*	0.424	0.997	0.959
Eur.	Extns	✗	✗	✗	13	16	0.159	0.265	0.999	0.987	0.221	**0.044**	0.992	0.997
NW	All	✓	✓	✗	23	25	0.335	0.060*	0.385	0.996	0.354	0.075*	0.975	0.830
NW	All	✗	✓	✗	23	24	0.377	**0.014**	0.977	0.996	0.283	0.099*	0.621	0.840
NW	All	✗	✗	✓	16	27	0.215	0.088*	0.943	0.960	0.382	0.231	0.775	0.865
NW	All	✗	✗	✗	16	27	0.528	0.128	0.919	0.608	0.347	0.055*	0.883	0.899
NW	Extns	✗	✗	✓	13	17	**0.034**	**0.041**	0.848	0.929	0.111	0.124	0.943	0.956
NW	Extns	✗	✗	✗	13	17	**0.041**	**0.026**	0.636	0.967	0.094*	0.061*	0.986	0.952
Pre-LGM	All	✓	✓	✗	18	20	0.432	0.993	0.987	0.977	0.958	0.942	0.990	0.682
Pre-LGM	All	✗	✓	✗	17	19	0.918	0.966	0.999	0.611	0.961	0.879	0.999	0.818
Pre-LGM	Extns	✗	✗	✓	8	12	0.648	0.763	0.918	0.790	0.641	0.902	0.964	0.679
Pre-LGM	Extns	✗	✗	✗	8	12	0.688	0.743	0.999	0.641	0.999	0.944	0.999	0.842